

IRAF Lab – 2

Aim:

To perform cosmic ray correction on images, obtain statistics of images, shifting and co-addition of images using various tasks on IRAF.

Introduction:

Cosmic Ray Correction is crucial in maintaining the accuracy of CCD observations. When the CCD is exposed to capture astronomical images, cosmic rays can leave distinct signatures, typically one pixel or a small cluster with unusually high values. These signatures, unlike the spread-out light from astronomical sources, can lead to erroneous source detections and inaccurate photometric results if not properly addressed.

Understanding Image Statistics provides valuable insights into various parameters, such as pixel value variations and overall pixel count. This statistical information is essential for gaining a comprehensive understanding of the characteristics of the captured images.

Image Shifting is a technique that involves adjusting the x, y coordinates of a point within a frame. This capability proves useful in aligning objects to specific pixels, simplifying tasks like co-adding and cross-matching using x, y coordinates.

Co-adding, the process of combining multiple image frames, is employed to enhance the Signal-to-Noise Ratio (SNR). By co-adding frames, the resulting image quality is improved, contributing to more reliable and precise data analysis in astronomical observations.

Procedure:

1. Cosmic Ray Correction:

The correction for cosmic rays was carried out using the '**cosmicrays**' task from the IRAF's **noao.imred.crutila** package, with default parameter values applied. To streamline the correction process across all provided files, a file list was generated through the command '**ls fs*.fit > filelist**' in the terminal.

The '**epar**' command was then used to modify the input parameter of '**cosmicrays**' to '**@filelist**,' and the output was adjusted to '**cr_//@filelist**'.

The subsequent images portray the discernible impact of cosmic ray correction on selected images. To facilitate a clear comparison of correction effects, the scale and colorbars were standardized across both frames.

Upon closer inspection, a distinct difference becomes apparent: prior to correction, numerous small bright pixels, corresponding to the characteristic signature of cosmic rays hitting CCDs, are visible in the images, while these are notably absent in the corrected versions.

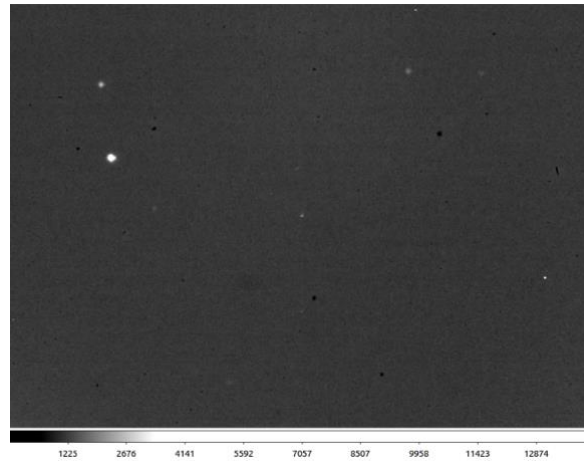
This process aids in enhancing the overall quality and reliability of the astronomical image data.

Below are a set of images before and after cosmic correction.

Image fs24_50s_J_set1_1.fits



Before cosmic ray correction

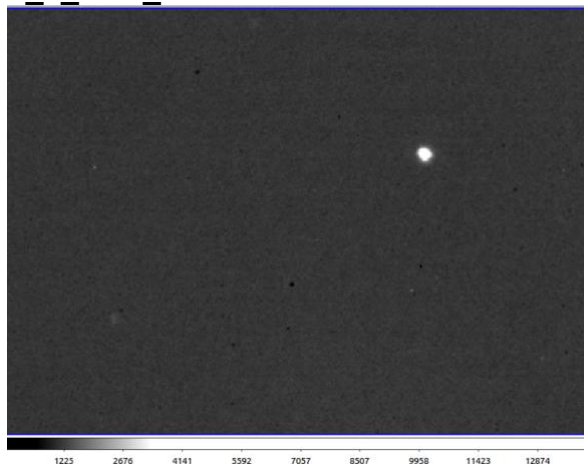


After cosmic ray correction

Image fs24_50s_J_set3_2.fits



Before cosmic ray correction

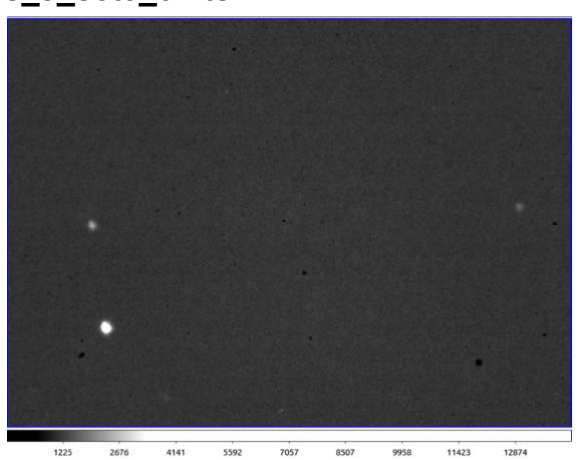


After cosmic ray correction

Image fs24_50s_J_set5_3.fits



Before cosmic ray correction



After cosmic ray correction

2. Image Statistics

The statistical analysis of the images was conducted using the 'imstat' task from the IRAF's images.imutil package. This task provided crucial information about various parameters characterizing the pixel distribution within the images.

To streamline the statistical assessment for all images simultaneously, the input for the 'imstat' task was configured as '@cr_//filelist.' This approach allowed for the efficient extraction of statistics for each image in one consolidated operation.

The focus of the statistical computations was specifically on the cosmic ray corrected images. This targeted analysis ensured that the obtained statistics accurately reflected the characteristics of the images without being influenced by the presence of cosmic rays, providing a more reliable basis for subsequent analysis and interpretation.

The resulting output featured several columns, each serving to describe different aspects of the images:

- ****image:**** Identifying the name of the image.
- ****npix:**** Indicating the number of pixels considered for the statistical analysis.
- ****mean:**** Representing the average value within the pixel distribution.
- ****stddev:**** Signifying the standard deviation, offering insights into the spread of pixel values.
- ****min:**** Denoting the minimum pixel value in the distribution.
- ****max:**** Highlighting the maximum pixel value in the distribution.

This comprehensive set of statistics contributes to a thorough understanding of the characteristics of the cosmic ray corrected images.

3. Image Shifting

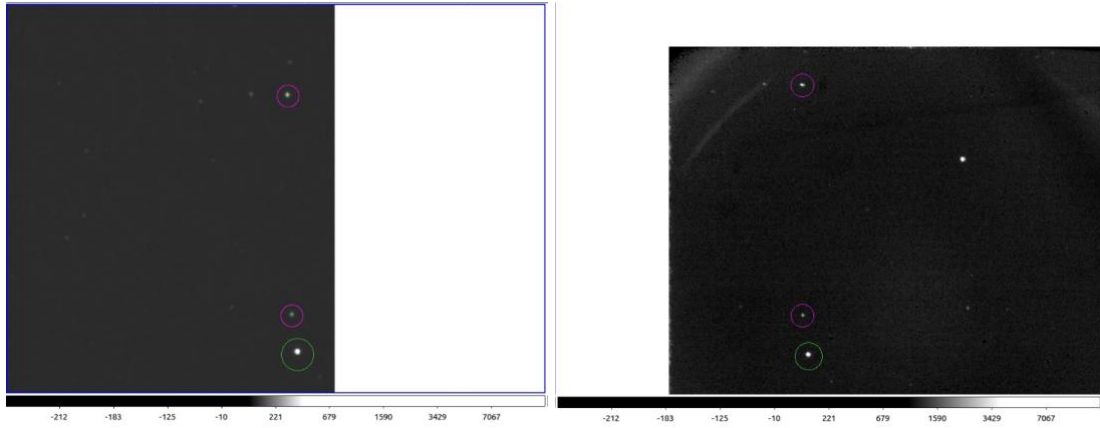
- The JHK magnitudes of star FS24 from the 2MASS All Sky Catalog are **J: 10.889 ± 0.023 mag, H: 10.811 ± 0.027 mag, and K: 10.769 ± 0.026 mag.**

- Multiple observations were conducted to facilitate **dithering**, a technique addressing issues like bad pixels, artifact detection, and compensating for flat-field effects, while efficiently sampling the background.

- Celestial coordinates for FS24 from the UKIRT catalogue are **RA(1950): 14 37 33.3** (in hms) and **Dec(1950): +00 14 36** (in dms).

- The image below provides a zoomed-in view of the 2MASS J frame containing FS24 (left) and another frame (right), with marked stars aiding in identification.

This visualization enhances understanding of the star's position and context within the observed field.



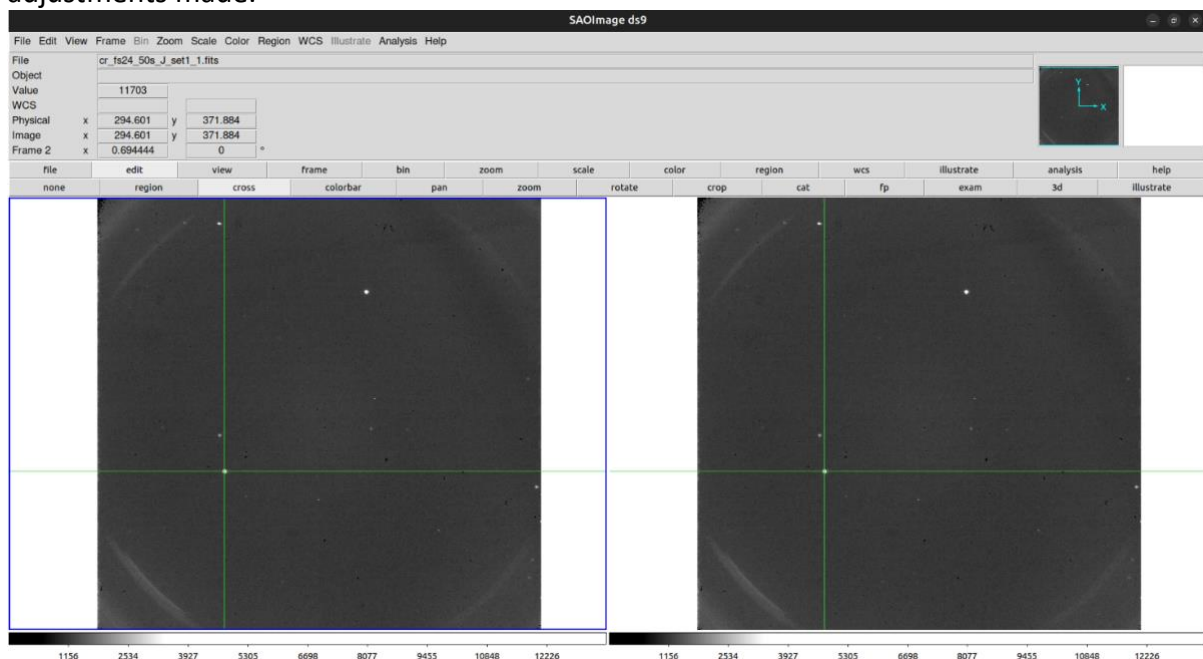
Green circle: used to mark FS24
Pink circle: used to mark other stars in the frame

To reposition the images, the '**imexamine**' tool was employed to determine the x,y coordinates of FS24 across all images. These coordinates were then utilized to generate a list of x,y shifts by subtracting each x,y position from the corresponding coordinates of FS24 in the initial image.

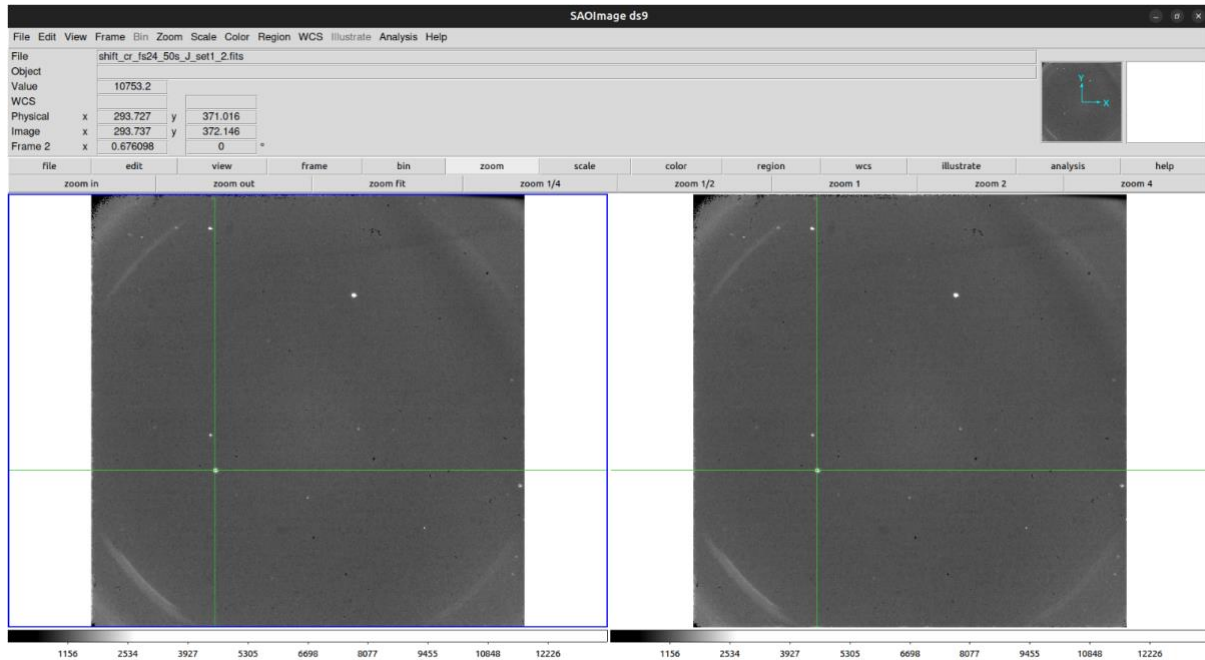
The resulting shift information was saved in ASCII table format under the filename '**imshift_ip.txt**'.

Subsequently, the '**imshift**' task was implemented to apply these shifts uniformly across all images. The input parameter was configured as '**cr_//@filelist**', and the output was set to '**shift_cr_//@filelist**'.

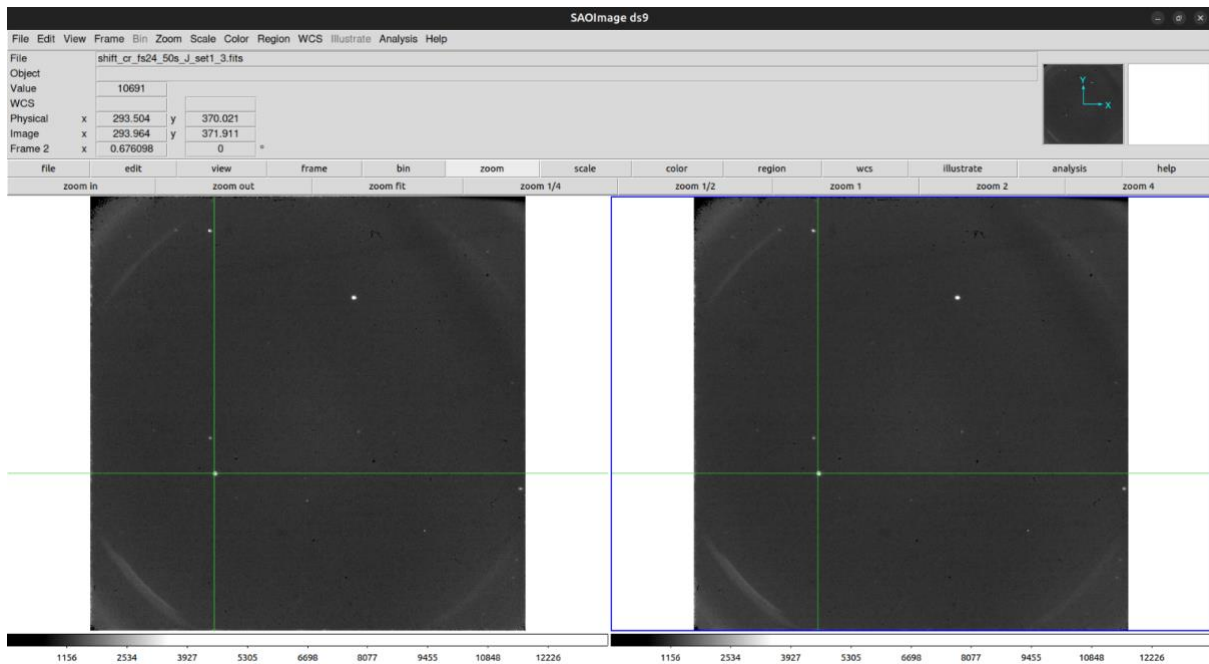
Additionally, the '**shift_**' parameter was specified as '**imshift_ip.txt**', allowing for the simultaneous application of shifts to all images. The images before and after this shifting process can be observed in the following pages for a visual representation of the adjustments made.



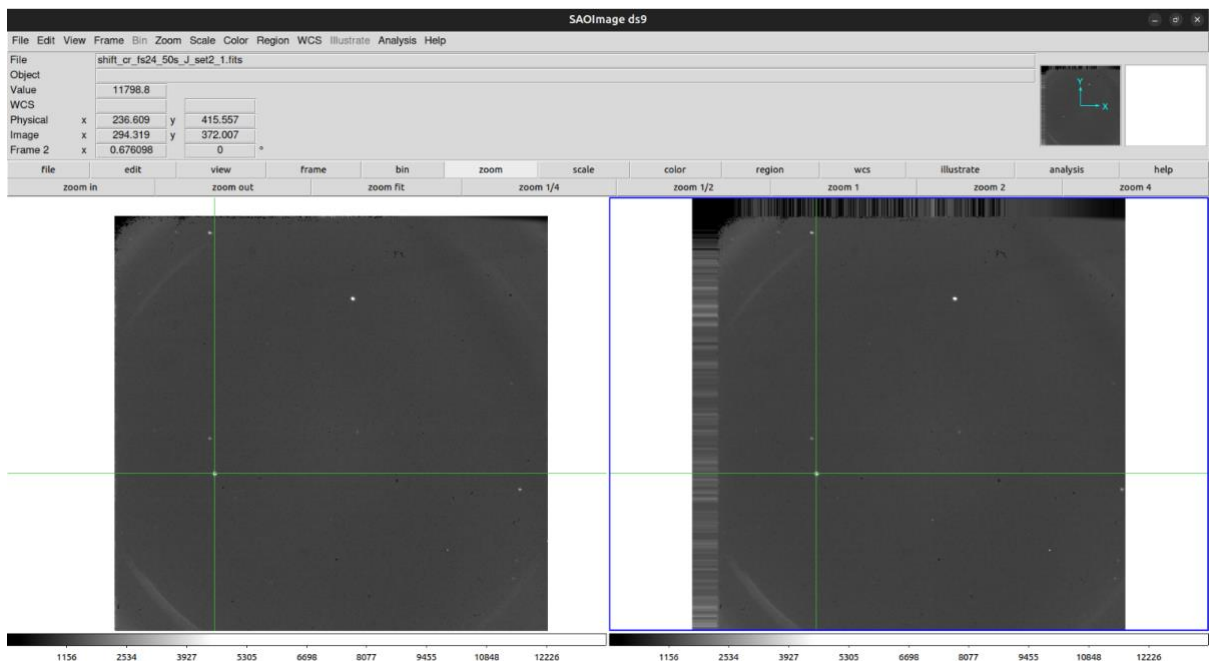
The image 'set1_1' is presented both before and after the shifting process. Since this image served as the reference, no actual shifting occurred. The crosshair denotes the approximate position of the reference star that was matched in all images.



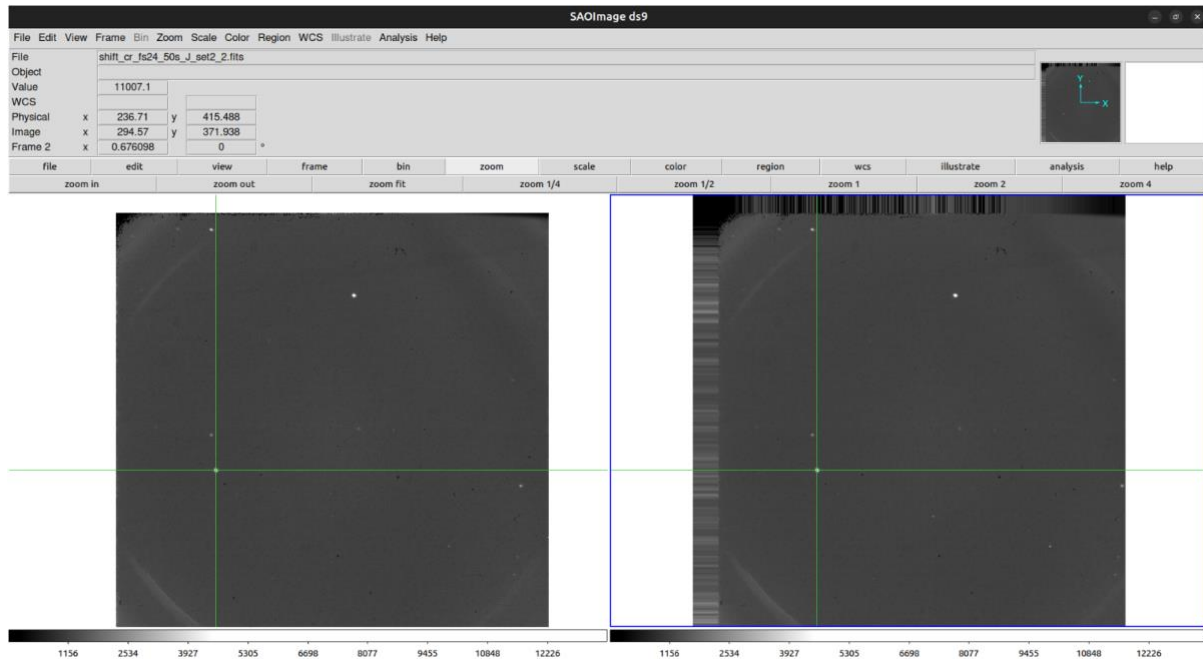
The 'set1_2' image is displayed before and after the shifting operation. Minimal x and y shifts were required for this particular image. The crosshair indicates the approximate position of the reference star that was matched in all images.



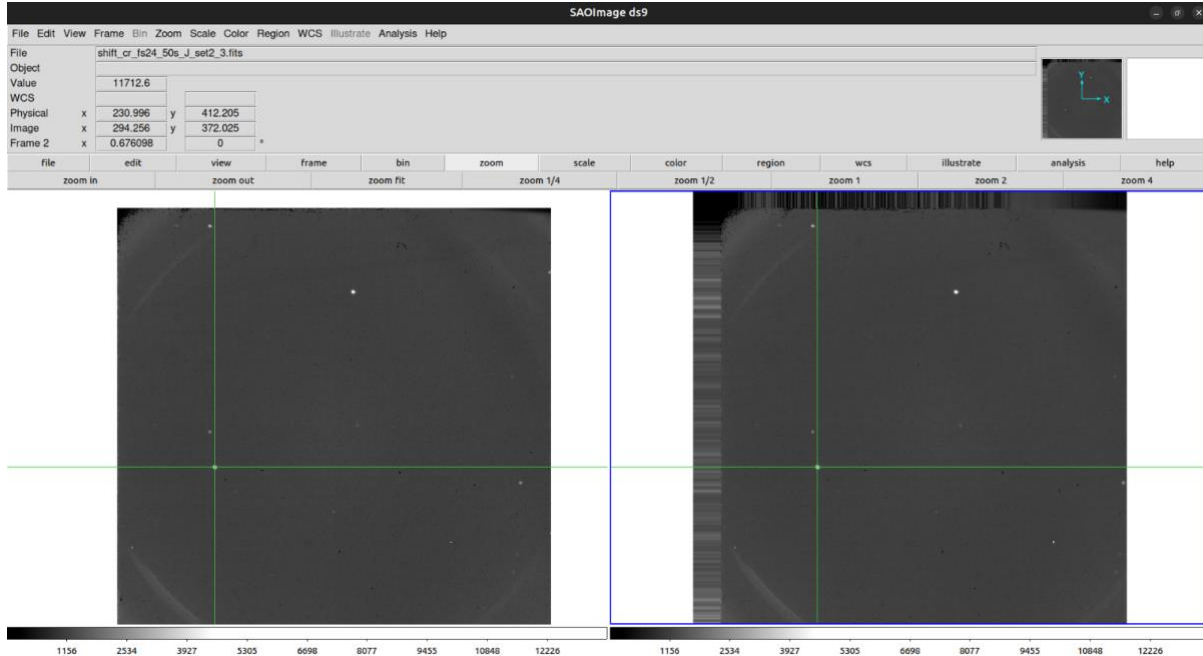
Displaying the 'set1_3' image before and after the shifting process, it required minimal x and y shifts. The crosshair marks the approximate position of the reference star that was matched in all images.



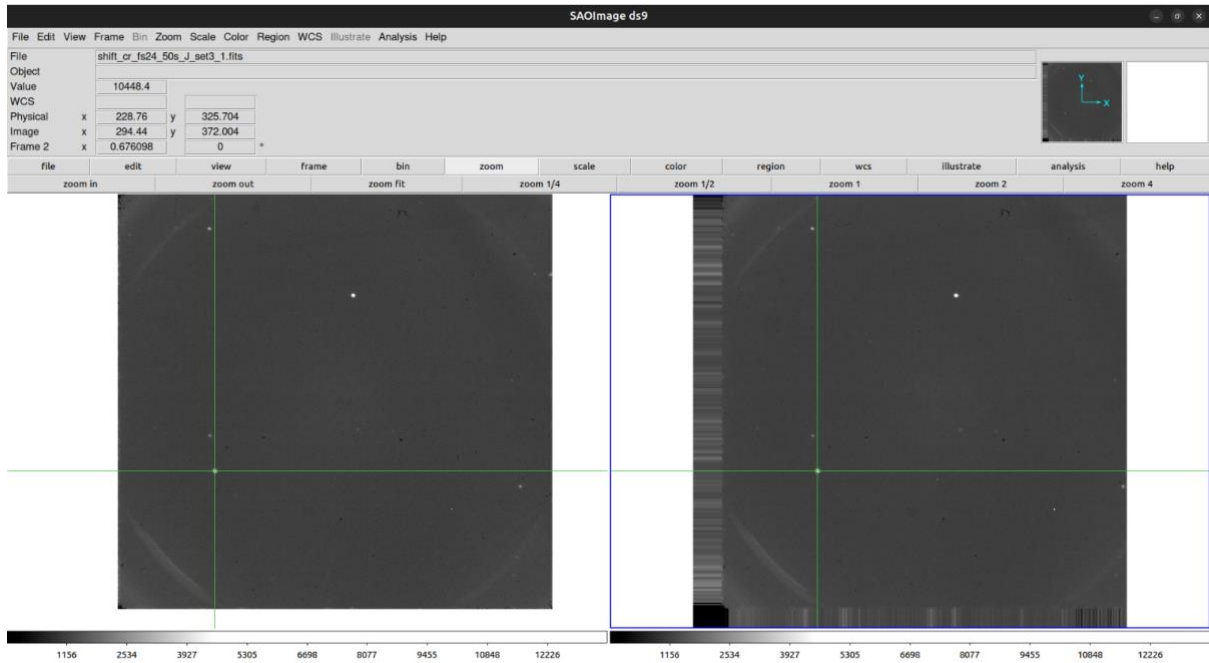
The 'set2_1' image is presented both before and after the shifting process, showcasing an expansion of the frame to accommodate the x and y shifts. The crosshair marks the approximate position of the reference star matched in all images. A noticeable difference in the physical and image coordinates of the reference star is evident.



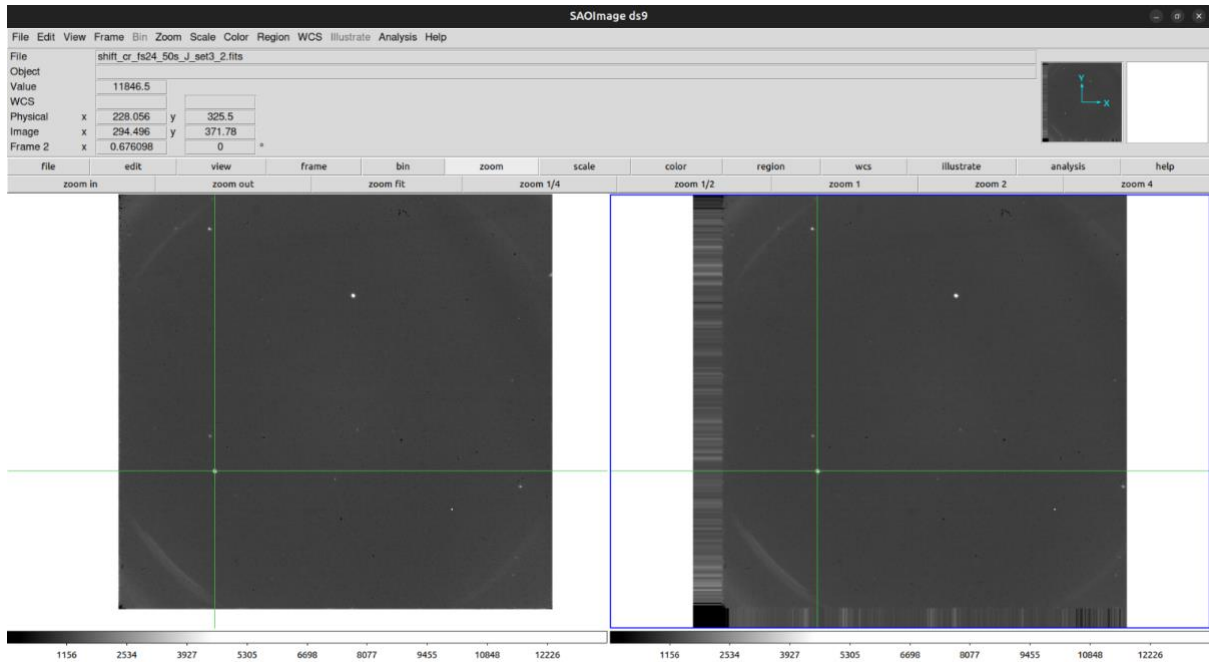
The 'set2_2' image is depicted before and after the shifting process, illustrating an expansion of the frame to account for the x and y shifts. The crosshair designates the approximate position of the reference star matched in all images. A noticeable distinction in the physical and image coordinates of the reference star is observable.



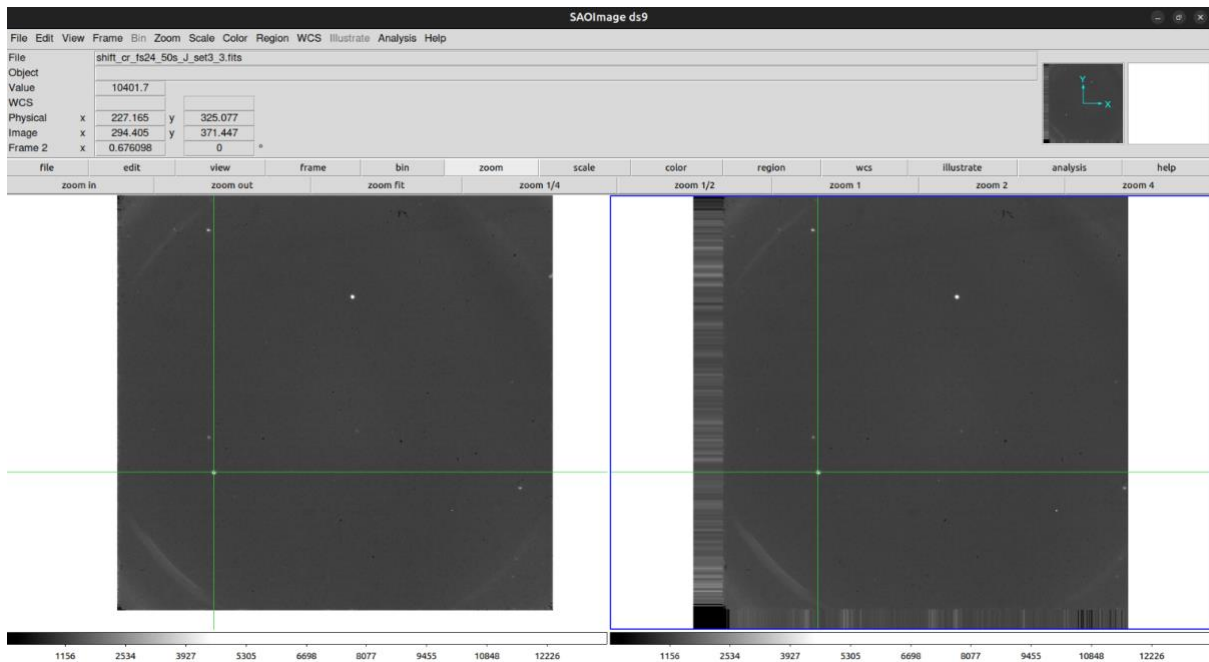
The 'set2_3' image before and after shifting. We can see that the size of the frame was increased to accommodate the x and y shifts. The approximate position of reference star that was matched was all images has been marked using the crosshair. We can clearly see a difference in the physical and image coordinates of the reference star.



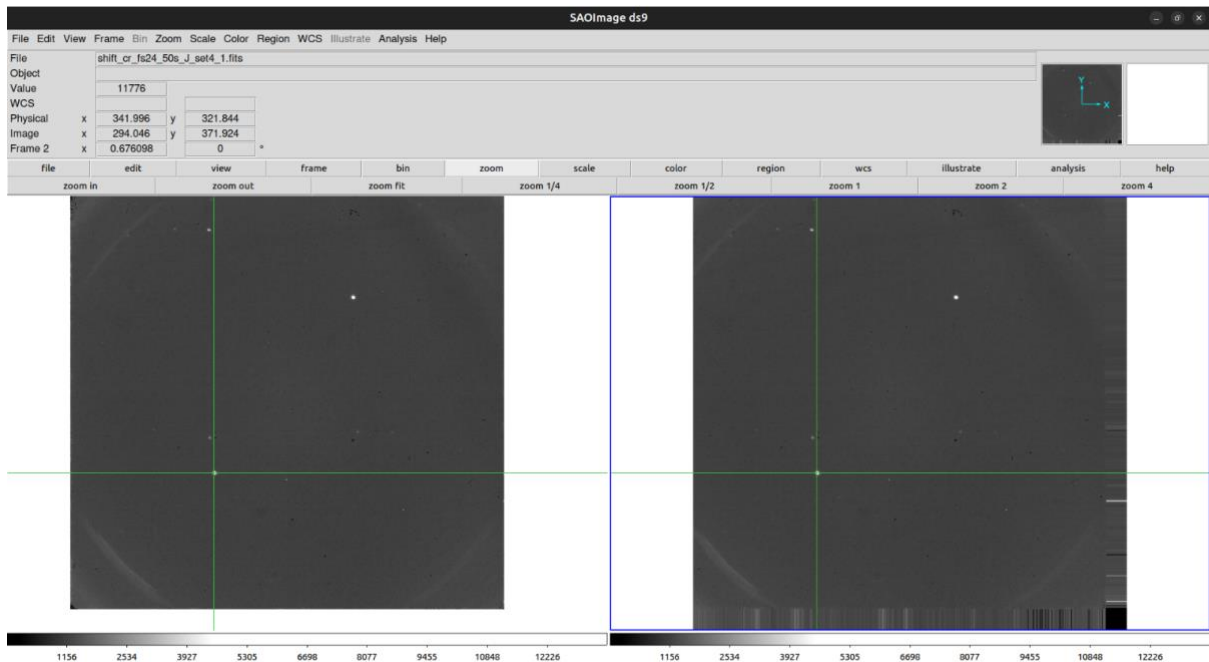
The 'set3_1' image is presented before and after the shifting process, with a noticeable expansion of the frame to accommodate the x and y shifts. The crosshair indicates the approximate position of the reference star matched in all images. A distinct disparity in the physical and image coordinates of the reference star is apparent.



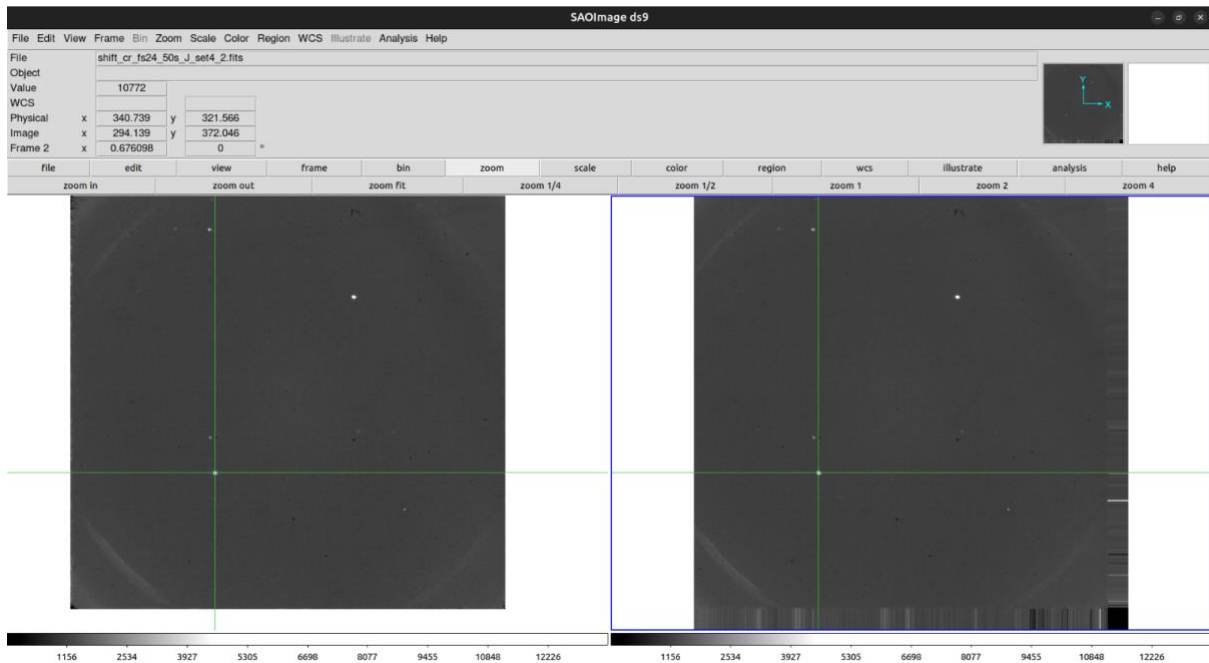
The 'set3_2' image is showcased before and after the shifting process, with an evident enlargement of the frame to adapt to the x and y shifts. The crosshair signifies the approximate position of the reference star matched in all images. A distinct variance in the physical and image coordinates of the reference star is clearly visible.



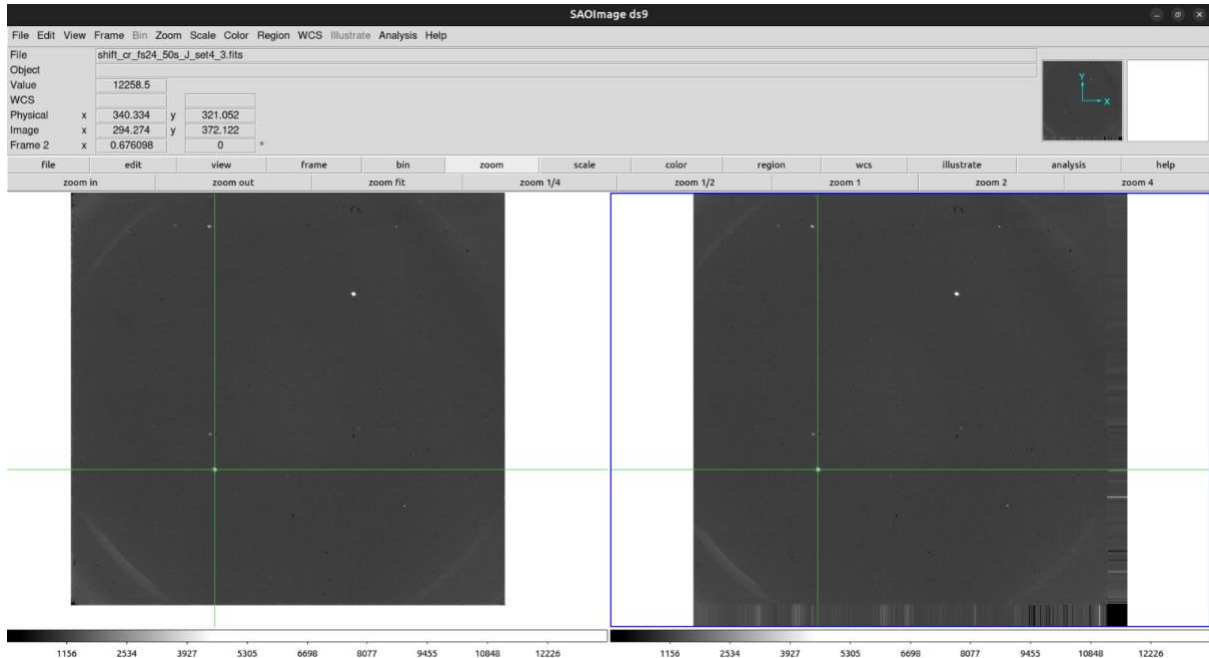
The 'set3_3' image is displayed both before and after the shifting process, revealing an expansion of the frame to adjust for the x and y shifts. The crosshair denotes the approximate position of the reference star matched in all images. A distinct contrast in the physical and image coordinates of the reference star is evident.



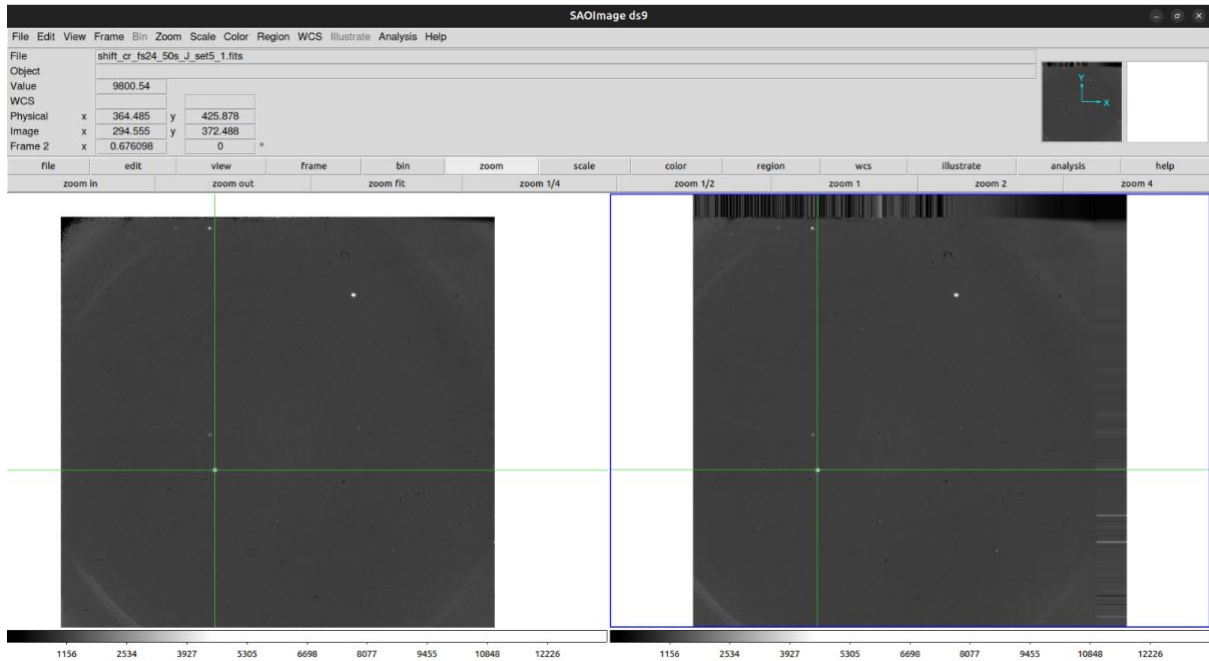
The 'set4_1' image is presented both before and after the shifting process, indicating an expansion of the frame to account for the x and y shifts. The crosshair designates the approximate position of the reference star matched in all images. A noticeable distinction in the physical and image coordinates of the reference star is clearly visible.



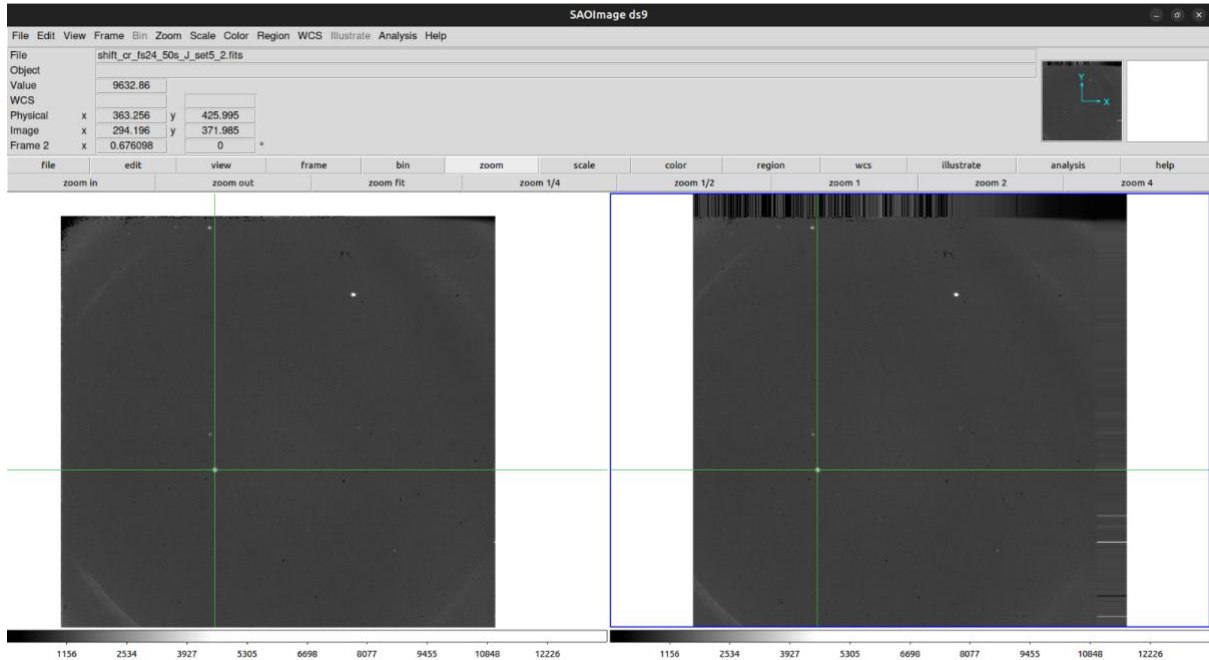
The 'set4_2' image is showcased both before and after the shifting process, revealing an enlargement of the frame to accommodate the x and y shifts. The crosshair designates the approximate position of the reference star matched in all images. A distinct difference in the physical and image coordinates of the reference star is clearly evident.



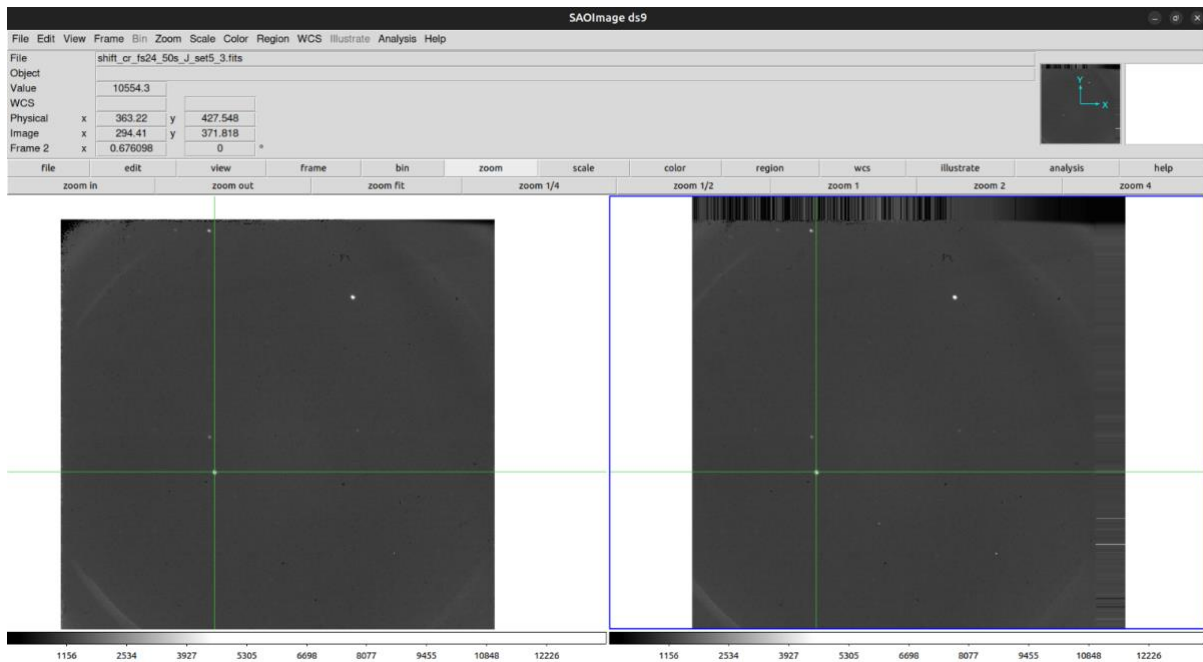
The 'set4_3' image is displayed both before and after the shifting process, illustrating an expansion of the frame to accommodate the x and y shifts. The crosshair indicates the approximate position of the reference star matched in all images. A noticeable difference in the physical and image coordinates of the reference star is clearly visible.



The 'set5_1' image is presented both before and after the shifting process, showcasing an enlargement of the frame to adjust for the x and y shifts. The crosshair designates the approximate position of the reference star matched in all images. A distinct contrast in the physical and image coordinates of the reference star is clearly visible.



The 'set5_2' image is showcased both before and after the shifting process, revealing an expansion of the frame to accommodate the x and y shifts. The crosshair designates the approximate position of the reference star matched in all images. A distinct difference in the physical and image coordinates of the reference star is clearly evident.

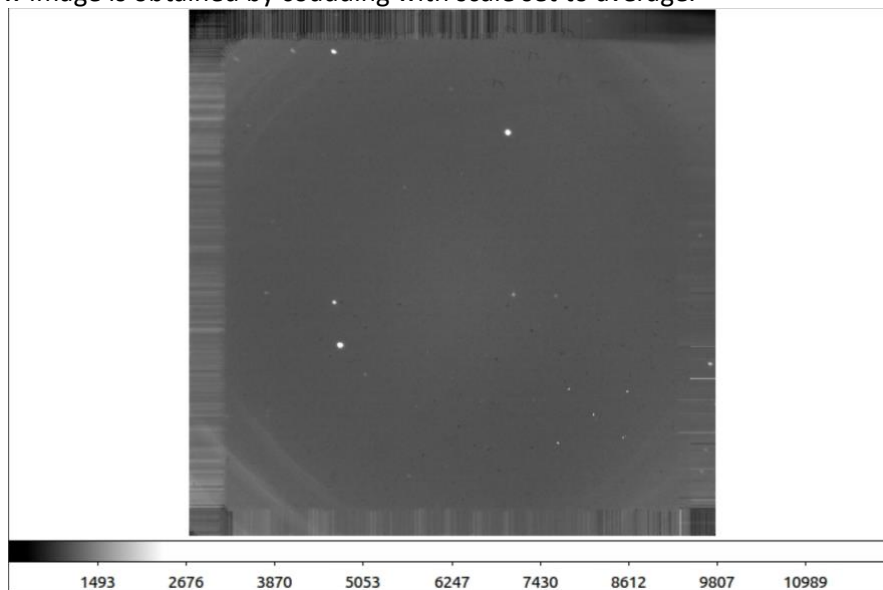


The 'set5_3' image is displayed both before and after the shifting process, illustrating an enlargement of the frame to accommodate the x and y shifts. The crosshair indicates the approximate position of the reference star matched in all images. A noticeable difference in the physical and image coordinates of the reference star is evident.

4. Co-Adding

The process of co-adding was executed using the '**imcombine**' task within the '**images.immatch**' package. The input parameter was configured as '**shift_cr_//@filelist,**' while the output parameter was set to '**avg_coadded.fits,**' and the combine parameter was specified as '**average**'.

The below image is obtained by coadding with scale set to average.



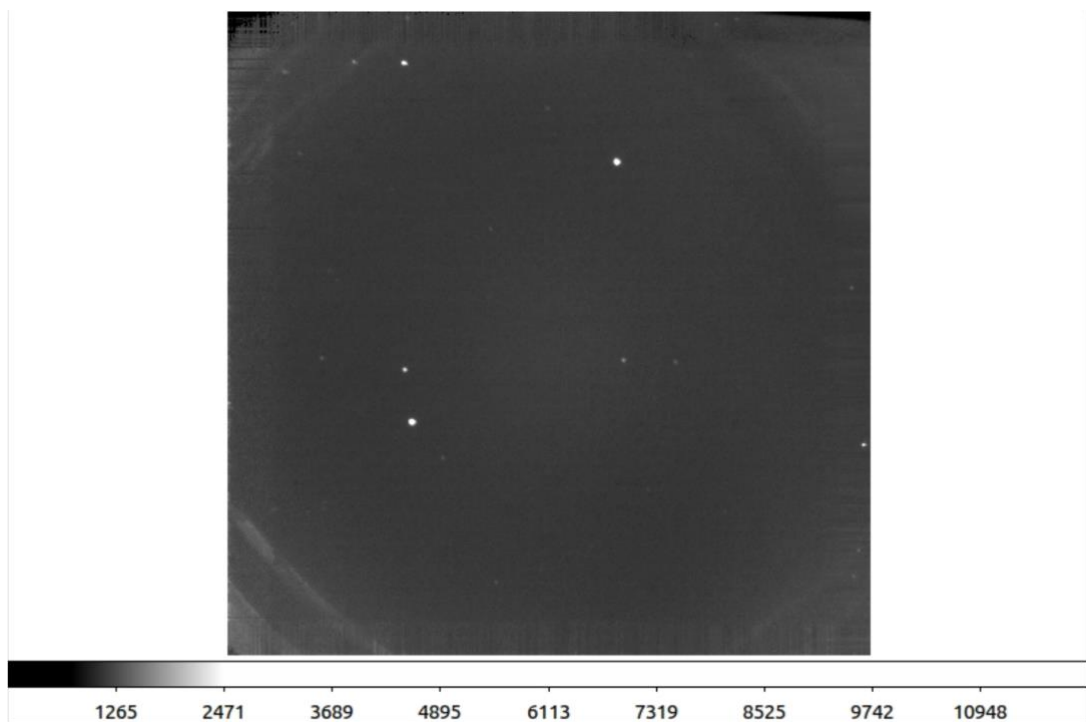
Upon examining the statistics of the median-combined image through the 'imstat' task, the following results are obtained:

Table

To perform median combining, the input parameter was configured as 'shift_cr_//@filelist'.

The output parameter was set to 'median_coadded.fits', and the combine parameter was specified as 'median'.

The result of this 'median' combination produced the following image.



On checking the statistics of the median combined image using the 'imstat' task, we get the following result,

*****Table*****

- This demonstrates that median combining yields a smoother image with a reduced standard deviation.
- Median combining is recognized for its ability to:
- Eliminate the effects of bad pixels.
- Address the impact of cosmic rays (not applicable here since those were already removed).
- Mitigate the effects of shooting stars, satellites, etc., entering the frame.

- Let's assume that the noise is primarily influenced by source noise, background noise, and dark noise, all known to follow a Poissonian distribution.

If we co-add n frames by either taking the sum or the average, the signal will increase by n times, assuming the images have similar exposure times.

However, since the noise is proportional to the square root of the sum of the source signal, background, and dark current, it will only increase by the square root of n .

Consequently, the Signal-to-Noise Ratio (SNR) will experience an increase on the order of the square root of n .

Conclusion:

After going through this tutorial on using IRAF to fix cosmic rays, gather image stats, shift images, and combine them, I now have a clearer understanding of how these tasks work and why they're important for organizing data.